AD-A065 159 INSTITUTE FOR ACOUSTICAL RESEARCH MIAMI FLA F/G 20/1
EXPERIMENTAL EVIDENCE OF THE IMPORTANCE OF SUB-BOTTOM REFRACTIO--ETC(U)
SEP 78 B ROSENBERG, L DOMINIJANNI, W JOBST N62269-75-C-0305
UNCLASSIFIED IAR-79001 NL

1 OF 1
ADA
065159

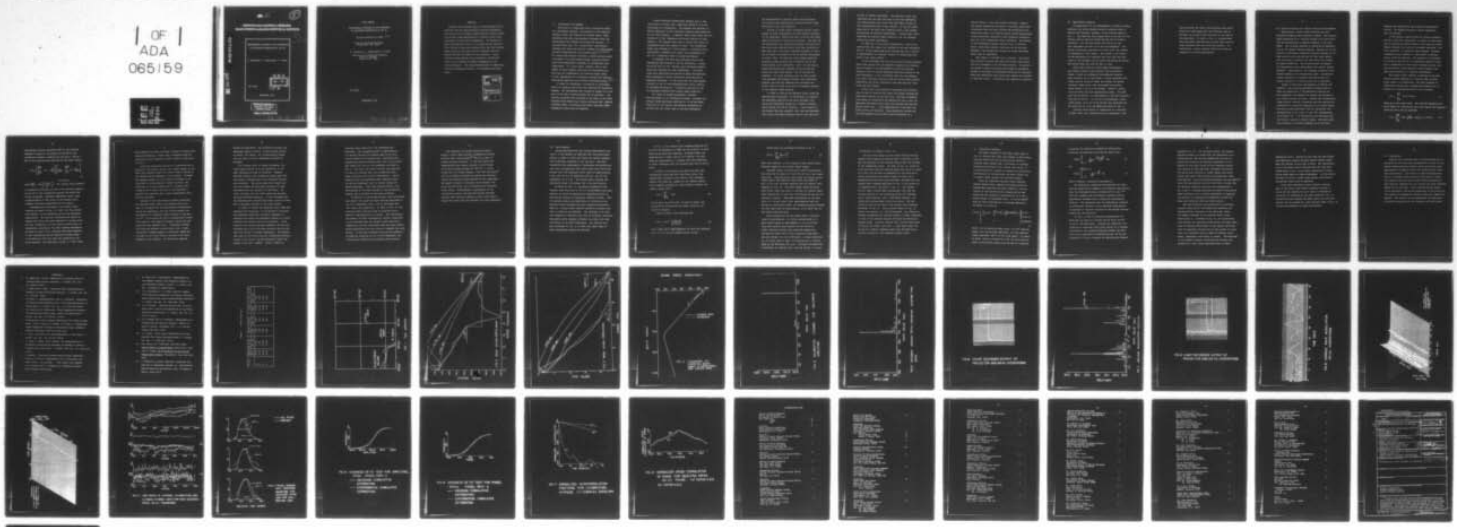

END
DATE
FILMED
4-79
DDC

LEVEL II

5

INSTITUTE FOR ACOUSTICAL RESEARCH
MIAMI DIVISION PALISADES GEOPHYSICAL INSTITUTE

See 1473 in back

EXPERIMENTAL EVIDENCE OF THE IMPORTANCE OF SUB-BOTTOM REFRACTION AT 206 HZ

B. Rosenberg, L. Dominijanni, W. Jobst

IAR 79001

September 1978

Miami, Florida 33130

FINAL REPORT

EXPERIMENTAL EVIDENCE OF THE IMPORTANCE OF SUB-BOTTOM REFRACTION AT 206 HZ

Contract N62269-75-C-0305

Naval Air Development Center
Warminster, Pa. 18974

B. Rosenberg, L. Dominijanni, W. Jobst

Institute for Acoustical Research
615 S.W. 2nd Ave.
Miami, Fla. 33130

IAR 79001

September 1978

Abstract

Acoustic data obtained using a bottom mounted 206 Hz projector and two bottom mounted receiving hydrophones 8.5 km and 21.8 km distant showed multiple acoustic paths with travel times approximately 30 percent faster than predicted for water-borne propagation. The presence of amplitude modulation with a 6.5 second period indicated that acoustic energy was reflected from the ocean surface before entering the high velocity limestone and coral bottom and being refracted to the receivers. Since received pulses showed little distortion, sub-bottom layers may be modeled as complex impedances at the 206 Hz frequency. The results demonstrate the importance of bottom propagated energy at low frequency and short range.

I. Introduction and Summary

When sound is transmitted from a stationary source to a stationary receiver, fluctuations in the received acoustic signal are observed as internal waves, tides, turbulence and other oceanographic processes alter the sound speed field between the source and receiver. It has been shown that, for a single path, fluctuations increase with range and provide a measure of oceanographic activity integrated over the acoustic path.[1,2,3,4,5] For source and receiver locations in which multiple paths are present, the relationship between acoustic fluctuations and oceanographic processes is considerably more complicated. It is well known, however, that if the number of paths becomes large and the fluctuations on each path are independent, the received signal field is well represented as a stochastic process with Rayleigh distributed amplitude and uniformly distributed phase.[6,7]

In order to investigate fluctuations on individual paths, an acoustic test range was installed off Eleuthera, Bahamas. Two hydrophones were located at ranges of 8.5 km and 21.8 km from a bottom mounted 206 Hz projector. The receiver locations were selected on the basis of ray trace analyses which showed that totally refracted (RR), surface reflected (RSR), and surface and bottom reflected (SRBR) propagation paths could be expected.

A phase modulated pseudorandom sequence with a time resolution of 20 msec and a repetition period of 9.94 sec was chosen for transmission. The sequence was designed to permit separation of the individual acoustic paths predicted by ray trace analysis. A computer based field system was configured to filter, demodulate and record signals on three channels. Two channels were used to record the outputs of hydrophones which were cabled to shore. The transmitted signal was recorded on a third channel, a procedure which established a reference for travel time measurements as well as a convenient check on system performance.

In December 1976 data were obtained from the two hydrophones and returned to IAR for processing. During the first half of 1977, acoustic path structure measurements were obtained for both hydrophones. Individual paths were identified and records of phase and amplitude were processed to obtain statistical distributions of amplitude and phase. It was noted that the time between arrivals on the 21.8 km hydrophone bore little relation to the model predictions. In addition one path to the far hydrophone demonstrated unusual phase stability.

As a check on system performance, analyses were performed on the calibration channel. Although the channel showed amplitude stability of .01 dB and phase stability of .001 radian, the detailed processing indicated that the travel time to the near hydrophone

was approximately 30 percent faster than predicted, and no paths were observed with travel times near those predicted by ray trace analysis.

Because of these highly unexpected results, which seemed in sharp disagreement with the physical geometry of the experiment, checks were made to verify the hydrophone and projector installation accuracy. The ship log and discussions with shipboard personnel indicated that the source and receivers should have been installed no more than 200 m from their intended locations, an error far too small to account for the 30 percent discrepancy in travel time. To check the field system operation, personnel present during data collection set up the field system in the laboratory. Data with the anticipated path delays were recorded on analog tape and played into the field system. The processing was repeated. All tests indicated that the data collection equipment and analysis software were operating properly and that the observed path structure was either correct or due to an error in hardware external to the computer based recorder.

In order to confirm the measured travel times and observed path structures, it was decided to reinstall the hydrophone amplifiers and shore equipment and record the hydrophone outputs on a Sanborn recorder while pulsing the 206 Hz projector. Since funds for the project had been expended, this test was postponed until early 1978 when personnel were at the test site

as part of another experiment. The results of this test indicated that the path structure to the near hydrophone was indeed correct and travel time was within 20 msec of that observed more than a year earlier. At the far hydrophone two of the paths were observed within a few hundred milliseconds of previous measurements. A third path, which exhibited the greatest phase stability, was not observed during the pulsed experiments.

In addition to the pulsed transmission, a 206 Hz continuous wave (cw) signal was recorded at the near hydrophone. The c.w. signal showed amplitude fluctuations with a period of approximately 6.5 seconds, typical of reflections from waves on the ocean surface.

It was concluded that the initial path structure measurements were correct with the possible exception of crosstalk being included in the measurements at the far receiver. Because of the 6.5 second amplitude modulation period at the near hydrophone, it was conjectured that the true propagation paths involved reflection from the ocean surface before penetrating and being refracted by the high velocity limestone and coral bottom.

In mid 1978 it was decided to reprocess the available data in hope of learning more about the unusual propagation conditions existing at the test site. New data thresholds were chosen to investigate the possibility that a very low amplitude water-borne path might have existed with the predicted travel time. A path approximately 16 dB below the first arrival was observed. Phase modulation records for this path showed that the path length fluctuated in a

similar manner to the high velocity arrivals. Despite the highly complex path structure, involving conjectured reflections from the ocean surface and penetration into sub-bottom layers, the received pulses showed surprisingly little distortion indicating little frequency dispersion over the 50 Hz transmitted signal bandwidth. The results of this experiment clearly indicate that, in shallow water, water-borne acoustic paths may not be the most energetic, and propagation through the ocean sub-bottom layers must be considered.

This report is divided into 6 sections. The source and receiver locations and predicted acoustic path structure are discussed in the following section. In section 3 the acoustic signal processing algorithms are presented. Records of the phase and amplitude stability of individual paths and comparisons with statistical models are included in sections 4 and 5. Conclusions are reported in section 6.

II. Experimental Geometry

In preparation for the measurements of acoustic channel stability two bottom mounted acoustic receivers were installed off Eleuthera, Bahamas, in the location shown in Fig. 1. The receivers were respectively 8.5 km and 21.8 km distant from an existing bottom mounted 206 Hz acoustic projector. The receiver depths were 1481 m for the near hydrophone and 4560 m for the far hydrophone. The source, previously installed on 26 June 1975, was located at approximately 290 m depth. The bottom in the region of the experiment was limestone and coral with new reef areas to the northwest of the source and behind the source. The bottom slope was from the west to east.

Based upon historical sound speed measurements, the nominal acoustic path structure was calculated. Figure 2 shows the bathymetry and predicted acoustic path structure to the near phone. Single refracted (RR), single surface reflected (RSR) and surface and bottom reflected (SRBR) paths were anticipated with travel times between 5.75 and 6.00 seconds. Predicted energy via RR and RSR paths was approximately equal. The SRBR path was estimated to be approximately 5 dB less energetic than the RR arrival. At the 21.8 km hydrophone, travel times between 14.69 and 14.82 seconds were predicted for the principal RR, RSR, and SRBR paths shown in Fig. 3.

Although measurements of temperature as a function of depth (XBT) were planned during the experiment, high

seas prevented the vessel from operating near shore. Historical sound speed data was therefore used to estimate the acoustic path structure at the time of the experiment. As shown in Fig. 4, limited sound speed estimates obtained from aircraft XBT's were in close agreement with the historical profile, Unfortunately, critical regions below 400 m were not examined by aircraft measurements.

III. Signal Processing for Channel Stability Measurements

Historically, acoustic path structure has been studied by dropping small explosive charges. The acoustic signal generated by an explosive charge is of short duration and approximates an impulse response in the time domain. The received waveform is therefore an approximation to the channel impulse response. Because of the difficulty in detonating successive explosive charges at the same location over long periods of time, short pulses from an acoustic projector are more useful for studies of channel stability. As the pulse-width is reduced, the transmitted signal approximates the channel impulse response. Unfortunately, low frequency projectors have limited bandwidth and limited peak power. Substantial signal processing is therefore required before the channel response to a single pulse can be extracted.

Based on theoretical developments by Metzger and Birdsall,[8] and previous experimental observations by Jobst and Dominijanni,[9] the modulation selected for this experiment was designed to measure the distortion on a single transmitted pulse. Rather than transmitting single pulses, however, processing gain was obtained by transmitting a repetitive sequence of 512 binary digits. The digits phase modulated a 206 Hz carrier with $+90^{\circ}$ corresponding to the digit "1" and -90° corresponding to the digit "0". The time duration of each digit was 19.4 msec or exactly 4 carrier cycles. The digit duration resulted in a signal bandwidth of 51.5 Hz and

equalled the bandwidth of the projector and matching network. The sequence duration, before repetition, was 9.94 seconds.

If the channel remains stable for several sequence periods, additional improvement in signal to noise ratio may be obtained by adding samples of the received signal complex envelope from several successive sequences. For this experiment, 16 sequences were averaged. Assuming independent noise samples, an improvement of approximately 12 dB was obtained. The operation is equivalent to filtering each of the 512 transmitted spectral lines with a narrowband 6.29 mHz filter centered on each line. The processing, called sequence block averaging, has been used extensively in previous experiments.

The channel digit response is defined as the time domain waveform observed at a receiver when a single pulse (digit) is transmitted. The digit response is obtained by noting that a transmitted sequence $s(t)$ of pulses $p(t)$ with modulation $d(\ell)$ may be written

$$s(t) = \sum_{\ell=0}^{511} d(\ell)p(t-\ell\Delta t) \qquad (1)$$

where Δt is the pulse width. The received sequence with pulse shape $a(t)$ modified by the ocean channel and sampled 4 times per digit may be expressed

$$r(i) = \sum_{\ell=0}^{511} d(\ell)\, a\left(\frac{i\Delta t}{4} - \ell\Delta t\right), \quad 0 \le i \le 2047. \qquad (2)$$

The discrete Fourier transform (DFT) of the received sequence is equal to the product of the DFT of the transmitted sequence, sampled once per digit, and the DFT of the received pulse modified by the ocean channel,

$$r(k) = \left[\sum_{\ell=0}^{511} d(\ell) \; W_{512}^{\ell k} \right] \left[\frac{1}{2048} \sum_{i=0}^{2047} a(i) \; W_{2048}^{ik} \right] \tag{3}$$

$0 \le k \le 2047,$

where $W_{512}^{\ell k} = \exp\left[\frac{-j \, 2\pi \ell k}{512} \right]$. The channel digit response is obtained by dividing the DFT of the received sequence by the DFT of the transmitted sequence and taking the inverse transform. Assuming independent noise, there is approximately 27 dB of gain in the channel digit response algorithm implemented with 512 digits.

Representative magnitudes of the channel digit response are shown in Figs. 5, 6 and 7 for the calibration channel, 8.5 km hydrophone and 22.8 km hydrophone respectively. The function illustrates the signal envelope which would have been observed if a single pulse had been transmitted, but the signal to noise ratio is considerably enhanced by the digit response processing. As shown in Figs 6 and 7, multiple paths were observed at both hydrophones and the separation between paths is considerably different from that predicted by ray trace analyses. The time axes in Figs. 5, 6 and 7 have

been segmented to show only those intervals in which major energy was observed. Travel time is measured from the occurrence of the calibration pulse, shown at "time zero" in Fig. 5.

Since the transmitted sequence is repetitive with a period of 9.94 seconds, travel time "wraps around" in the sense that acoustic paths with travel times in excess of one sequence period superpose on the display. Although the sequence length of 9.94 seconds was thought to be sufficient to avoid ambiguity between arrivals, the occurrence of a major energy peak 4.1 seconds after transmit with no major arrivals at the predicted 6 second delay indicated that a major experimental error may have occurred.

Because of the wide disparity between predicted and measured travel times, considerable effort was spent in validation of the experimental configuration. During the experiment, the time between samples was controlled by a frequency source accurate to one part in 10^{+8}. At the start of each 16 sequence data collection interval, the external frequency source was compared with the computer clock. Differences between the clock and external source greater than .6 msec, indicating a dropped sample or additional sample due to noise in the clock circuit, resulted in an error message on the teletype. No errors were reported

during the experiment. The calibration channel was amplitude stable to within .01 dB and phase stable to within .001 radian. All investigations showed that the data collection equipment performed as designed.

As a further check on signal processing, the field system was set up in the laboratory in the same configuration used at Eleuthera. Sequence generator outputs were recorded on analog tape with time delays corresponding to the estimated acoustic path structure. The analog tapes were played into the field system and digitized following the same procedures used for analysis of field data. All tests indicated that the field system and analysis software performed correctly. It was concluded that the observed path structure was either correct or else due to equipment external to the field system.

In order to confirm the measured travel times and observed path structures, it was decided to reinstall the hydrophone amplifiers and shore equipment at Eleuthera and record the hydrophone outputs on a chart recorder while pulsing the 206 Hz projector. Since funds for the project had been expended, the test was postponed until early 1978 when personnel were at the test site as part of another experiment. Two channels were used for recording with the transmitted pulse displayed on one channel and one hydrophone output displayed on the other channel. Figure 8 shows the

recorder output when the 8.5 km hydrophone was monitored. The transmitted pulse is approximately 0.2 seconds long and the leading edge of the first arrival appears 4.08 seconds later, consistent with experimental results obtained more than a year earlier. The results for the 21.8 km hydrophone are shown in Fig. 9. The first and second arrivals were observed 9.5 and 11.8 seconds after the transmitted pulse, again consistent with earlier measurements. The extremely stable high amplitude path observed during the initial experiment was not present during the pulsed experiment. This path occurred within a few milliseconds of the peak recorded on the calibration channel and is believed to have been crosstalk.

In addition to the pulsed carrier, chart recordings were made of the received signal envelope amplitude at the 8.5 km hydrophone when a 206 Hz continuous wave (cw) signal was transmitted. As shown in Fig. 10, the received signal envelope shows fluctuations with a period of approximately 6.5 seconds. The fluctuations are typical of those introduced by surface reflections. It was concluded that the acoustic paths were quite complex and involved reflections from the ocean surface before penetrating the high velocity limestone and coral bottom. It was also concluded that, with the exception of possible crosstalk on the 21.8 km hydrophone, the initial data recording and processing were correct.

The importance of bottom refracted acoustic energy in short range acoustic propagation has been noted by other investigators[10-13] and is a topic of current research interest. It has been shown that compressional wave energy striking a solid bottom at elevation angles between 70° and 90° is transmitted into the bottom sediment with high efficiency[14] and can be upward refracted to produce the energetic signals and multiple paths observed on this experiment. The speed of sound in limestone varies between 1700 m/sec and 4000 m/sec and is consistent with observed travel times. Unfortunately, confirmation of the conjectured surface reflected and bottom refracted acoustic path structure requires a more fully instrumented test range than was available for this experiment.

IV. Data Analysis

Having confirmed that the initial measurements were valid, it was decided to reprocess data from both hydrophones in order to learn more about the unusual propagation conditions existing at the test site. New data thresholds were programmed to investigate the possibility that very low amplitude water-borne paths might have been present with the predicted travel times of approximately 6 sec. for the 8.5 km hydrophone and 14.7 sec for the hydrophone at 21.8 km. The channel digit response was calculated every 9.94 minutes for a one day interval.

As shown in Fig. 11, successive estimates of the acoustic path structure at the 8.5 km hydrophone are quite similar, as would be expected for propagation which is principally through an unchanging limestone bottom. (The 6.5 second surface wave modulation is filtered by the sequence block averaging and digit response processing). Time for a single digit response estimate increases from left to right on the abscissa. The ordinate is in relative energy on a decibel scale with an arbitrary reference. Successive digit response estimates are shown with time increasing on the third coordinate. The abscissa has been truncated in Fig. 11 to show only those times at which significant energy was observed.

In Fig. 12 the channel digit response magnitude for the 21.8 km hydrophone is shown for the interval in which water-borne paths were expected. Although energy was observed with a travel time of 14.3 seconds, the path delay was approximately .4 seconds less than predicted, an error indicating that the observed path was not water-borne.

In order to investigate the phase and amplitude fluctuations associated with individual paths, time windows were selected in the channel digit response. Within each window W_s, samples of the complex channel digit response envelope M(j) were summed to produce the complex signal vector

$$g(i) = \sum_{j \in W_s} M(j) \qquad (4)$$

Signal power for each path, or group of paths, was estimated by multiplying the signal vector by its complex conjugate.

Phase estimates were obtained from

$$\theta(i) = \text{TAN}^{-1} \frac{\text{Im}\left[g(i)\right]}{\text{Re}\left[g(i)\right]} \qquad (5)$$

where $\text{Re}[g(i)]$ and $\text{Im}[g(i)]$ denote the real and imaginary parts of the windowed complex signal vector.

Noise power was estimated according to Eq. 6

$$n^2(i) = \sum_{j \epsilon W_n} \left| M(j) \right|^2 \qquad (6)$$

where the summation is in a region of the channel digit response judged not to contain signal energy.

Although signal to noise ratio varied considerably, the ratio was in excess of 10 dB for all but a few sample intervals. Representative time series for signal energy, signal phase, and signal-to-noise ratio are shown in Fig. 13 for four arrivals selected from the channel digit response in Fig. 11. The three higher amplitude paths with travel times less than 5.5 seconds all exhibit amplitude fluctuations of less than 4 dB during the one day observation interval. Amplitude fluctuations on the path with a 5.7 second travel time, approximately that predicted for water-borne paths, was somewhat greater although the path amplitude was approximately 16 dB below that of the bottom refracted path.

Phase records for the four paths show a long-term trend of approximately .25 cycles corresponding to a path length change of approximately 1.8 m in one day. Since the acoustic path analysis on the 206 Hz cw signal indicated surface wave amplitude modulation, the acoustic paths are at least partially water-borne and such changes are not unreasonable. A phase modulation of .22 cycles (peak to peak) is predicted due to surface tides at the Eleuthera test site. Although the modulation is difficult to identify with a one day record, a 12 hour

periodicity is evident in Fig. 13.

The very high signal to noise ratio obtained through channel digit response processing made it possible to compare the envelope of the received signals with the envelope of the transmitted signal. As shown in Fig. 13, signal to noise ratios for the four selected paths were often in excess of 10 dB, with the path corresponding to the water-borne travel time having the poorest signal-to-noise ratio. Representative received pulse envelopes, selected from the channel digit response magnitude in Fig. 11 and plotted on an expanded scale, are shown in Fig. 14. The largest arrival shows a pulse-width considerably less than the 20 msec duration of the calibration pulse and indicates that a second arrival, with a 180° phase reversal, cancelled the trailing edge of the first pulse. The cancellation can also be seen in the channel digit response magnitude in Fig. 11. Later arrivals shown in Fig. 14, showed time spreads of a few milliseconds. The similarity between transmitted and received pulses is rather remarkable in view of the probable surface reflected and bottom propagated paths. The data indicate that, had the sub-bottom structure been known, ray trace analyses which treat the bottom as a complex impedance might have provided satisfactory estimates of the received acoustic field.

V. Statistical Analysis

The phase records for individual paths shown in Fig. 13 indicate that long term changes in path length occurred during the one day observation interval. Although these changes make it difficult to estimate fluctuation statistics from limited time series, it is nevertheless of interest to examine the probability distributions of the amplitude and phase records and to compare these records with available models.

Since the individual acoustic paths examined through channel digit response processing exhibited considerable amplitude and phase stability, the statistics of the received digit response may be compared with the theoretical distributions of a sinusoidal signal in narrowband noise. It can be shown[15] that the joint distribution of envelope amplitude R and phase θ is given by

$$f(R,\theta)=\begin{cases} \dfrac{R}{2\pi\sigma^2}\exp\left[-\dfrac{R^2+A^2-2AR\cos(\theta-\psi)}{2\sigma^2}\right] & \begin{matrix}0\leq R<\infty\\ 0\leq\theta\leq 2\pi\end{matrix} \\ 0 & \text{elsewhere}\end{cases} \tag{7}$$

where ψ is an arbitrary phase angle, θ is the observed phase, R is the envelope amplitude, A is the constant signal amplitude, and σ^2 is the noise power. At signal to noise ratios in excess of 10 dB, the joint density takes a particularly simple form and may be integrated

to provide the cumulative probability distribution functions for amplitude alone and for phase alone,

$$F(R) \approx \int_{R'=-\infty}^{R} \frac{1}{\sqrt{2\pi}\sigma} e^{\frac{-[R'-A]^2}{2\sigma^2}} dR' \qquad (8)$$

and

$$F(\theta) \approx \int_{y=-\infty}^{\sqrt{2}\frac{R}{\sigma}\sin\theta} \frac{1}{\sqrt{2\pi}} e^{\frac{-y^2}{2}} dy, \qquad (9)$$

where F denotes a cumulative distribution.

The theoretical cumulative distributions for amplitude and phase may be compared with measured distributions using the Kolmogorov-Smirnov goodness-of-fit test.[16] This test compares the distribution obtained from the experimental ensemble with a theoretical distribution function. The hypothesis that the experimental ensemble is distributed according to the theorized distribution is accepted or rejected according to the maximum distance between the two functions.

In Figs. 15 and 16 cumulative distributions for amplitude and phase are plotted for the first arrival at the 5.8 km hydrophone. Although the cumulative distribution of amplitude seems quite similar to a Gaussian distribution, the maximum difference between the theoretical and experimental distributions was .08 and the probability of being incorrect by rejecting the Gaussian

hypothesis is .54. For the phase record, the maximum distance between the theoretical and experimental distributions was .061 and the probability of being incorrect by rejecting the Gaussian hypothesis is .83. Because of long term trends and low frequency modulation present in both amplitude and phase time series, the series were filtered to remove energy with periodicity less than 6 hours before the statistical tests were applied. Also the Kolmogorov-Smirnov test was applied using the experimental variance from Table 1 rather than the variance predicted from the noise backgrounds in Eq. 8 and 9. Although amplitude and phase flucatuations seem consistent with a Gaussian hypothesis as expected, the variance is increased by propagation through the water and reflection from the ocean surface.

The time stability of fluctuations on individual acoustic paths may be investigated by examining the autocorrelation functions of the amplitude, phase, and complex envelope of the received signal vector given by Eq. 4. As shown in Fig. 17, the autocorrelation function for amplitude fluctuations (the mean amplitude is removed) decorrelates in one sample indicating that the amplitude fluctuations at high signal to noise ratio are consistent with an additive Gaussian noise model, independent from sample to sample. The magnitude of the complex envelope autocorrelation reflects the presence of a mean signal amplitude which is large

compared to noise. Because of the large and very stable mean amplitude, complex envelope samples exhibit dependence for periods of more than 2 hours. The autocorrelation of the phase record indicates that the long term trends shown in Fig. 13 are quite significant in determining phase sample-to-sample dependence. (If the record had been filtered to remove these trends, much shorter correlation times would be expected).

Since paths apparently travel through a similar part of the water column before entering the high velocity bottom, modulation on all paths is expected to be similar as indicated by the phase records in Fig. 13. Crosscorrelations between the phase record for the first arrival and the records for later arrivals shown in Fig. 18 confirm the dependence of path fluctuations.

VI. Conclusions

Acoustic data obtained using a bottom mounted 206 Hz projector and two receiving hydrophones 8.5 km and 21.8 km distant showed multiple acoustic paths with travel times approximately 30 percent faster than predicted for water-borne propagation. The presence of amplitude modulation with a 6.5 second period indicated that acoustic energy was reflected from the ocean surface before entering the high velocity limestone and coral bottom and being refracted upward to the receivers. Since received pulses showed little distortion, sub-bottom propagation at 206 Hz may be well modeled as propagation through layers with complex impedance. The results clearly demonstrate the importance of bottom interactions at low frequency and short range.

References

1. W. Jobst and J. Clark, "Modulation of acoustic phase by internal-wave vertical velocity", J. Acoust. Soc. Am., 61, 688-693 (1977).
2. S. Adams and W. Jobst, "Estimation and interpretation of acoustic cw phase fluctuation spectra", J. Acoust. Soc. Am., 61, 675-681, (1977).
3. W. Jobst, X. Zabalgogeazcoa, and N.L. Weinberg, "Simulation of acoustic phase modulation by a first-mode directional internal wave", J. Acoust. Soc. Am., 61, 1163-1168 (1977).
4. W.H. Munk and F. Zachariasen, "Sound propagation through a fluctuating stratified ocean: theory and observation", J. Acoust. Soc. Am., 59, 818-837, (1976).
5. Fluctuations do not increase indefinitely but reach an upper bound. See S. Flatte, R. Dashen, W.H. Munk, F. Zachariasen, Sound transmission through a fluctuating ocean, Standford Research Institute, JSR-76-39, May 1977.
6. I. Dyer, "Statistics of sound propagation in the ocean", J. Acoust. Soc. Am., 48, 337-345 (1970).
7. F. Dyson, W. Munk, and B. Zetler, "An interpretation of multipath scintillations Eleuthera to Bermuda in terms of internal waves and tides", J. Acoust. Soc. Am., 59, 1121-1133, (1976).
8. K. Metzger, "Multipath studies using periodic sequences", Chapter 6 of Ph.D. dissertation, Univ. of Michigan, Ann Arbor, Mich., (in process).

The authors are indebted to K. Metzger and T.G. Birdsall for suggesting channel digit response processing.

9. W. Jobst and L. Dominijanni, "Measurements of the temporal spatial and frequency stability of an underwater acoustic channel", J. Acoust. Soc. Am., (accepted for publication).

10. R.E. Christensen, J.A. Frank, and W.H. Geddes, "Low-frequency propagation via shallow refraction paths through deep ocean unconsolidated sediments", J. Acoust. Soc. Am., 57, 1421-1426 (1975).

11. D.C. Stickler, "Negative bottom loss, critical-angle shift, and the interpretation of the bottom reflection coefficient", J. Acoust. Soc. Am., 61, 707-710 (1977).

12. R.R. Goodman and A.Z. Robinson, "Measurements of reflectivity by explosive signals", Physics of Sound in Marine Sediments, Vol. 1, p. 537-564, Plenum, New York (1974).

13. J.S. Hanna, "Short range transmission loss and evidence for bottom refracted energy", J. Acoust. Soc. Am., 53, 1686-1690 (1973).

14. W.M. Ewing, W.S. Jardetzky, and Frank Press, Elastic Waves in Layered Media, McGraw Hill, 1957.

15. John B. Thomas, An Introduction to Statistical Communication Theory, John Wiley & Sons, New York, 1969.

16. D. Middleton, Acoustic modeling, simulation and analysis of underwater targets, II. ARL-TR-69-22 Applied Research Laboratories, Univ. of Texas at Austin, Texas 78712.

Table 1 - 5-Mile Phone Data

Arrival	Amplitude in dB		Phase in Cycles		Signal to Noise in dB	
	Mean	Std. Dev.	Mean	Std. Dev.	Mean	Std. Dev.
A	49.46	0.524	.298	.107	24.02	3.19
B	37.96	1.30	.185	.113	13.21	2.97
C	38.08	0.934	.099	.121	12.53	2.30
D	33.44	1.943	-.016	.126	8.30	3.34

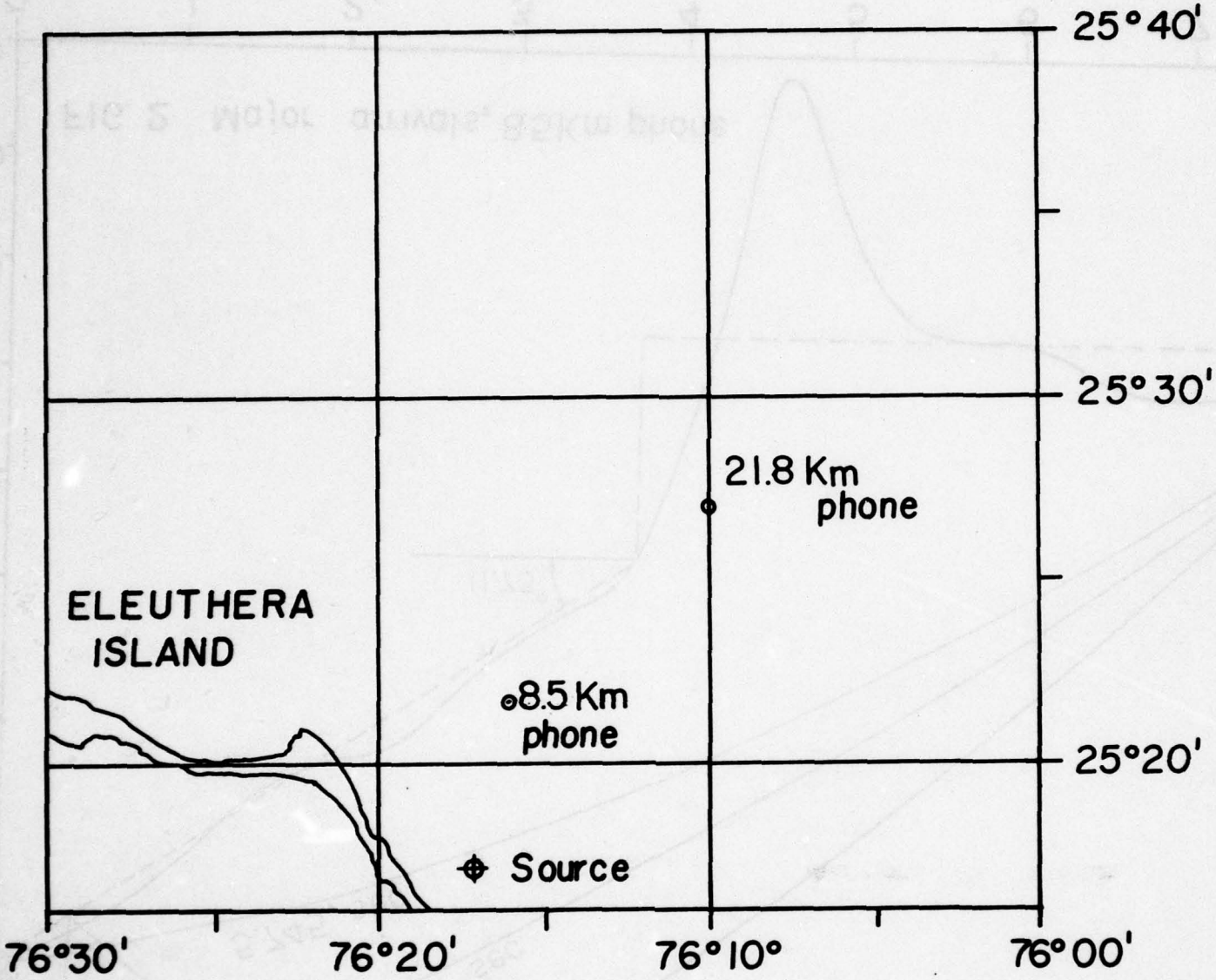

FIG. 1 Test geometry

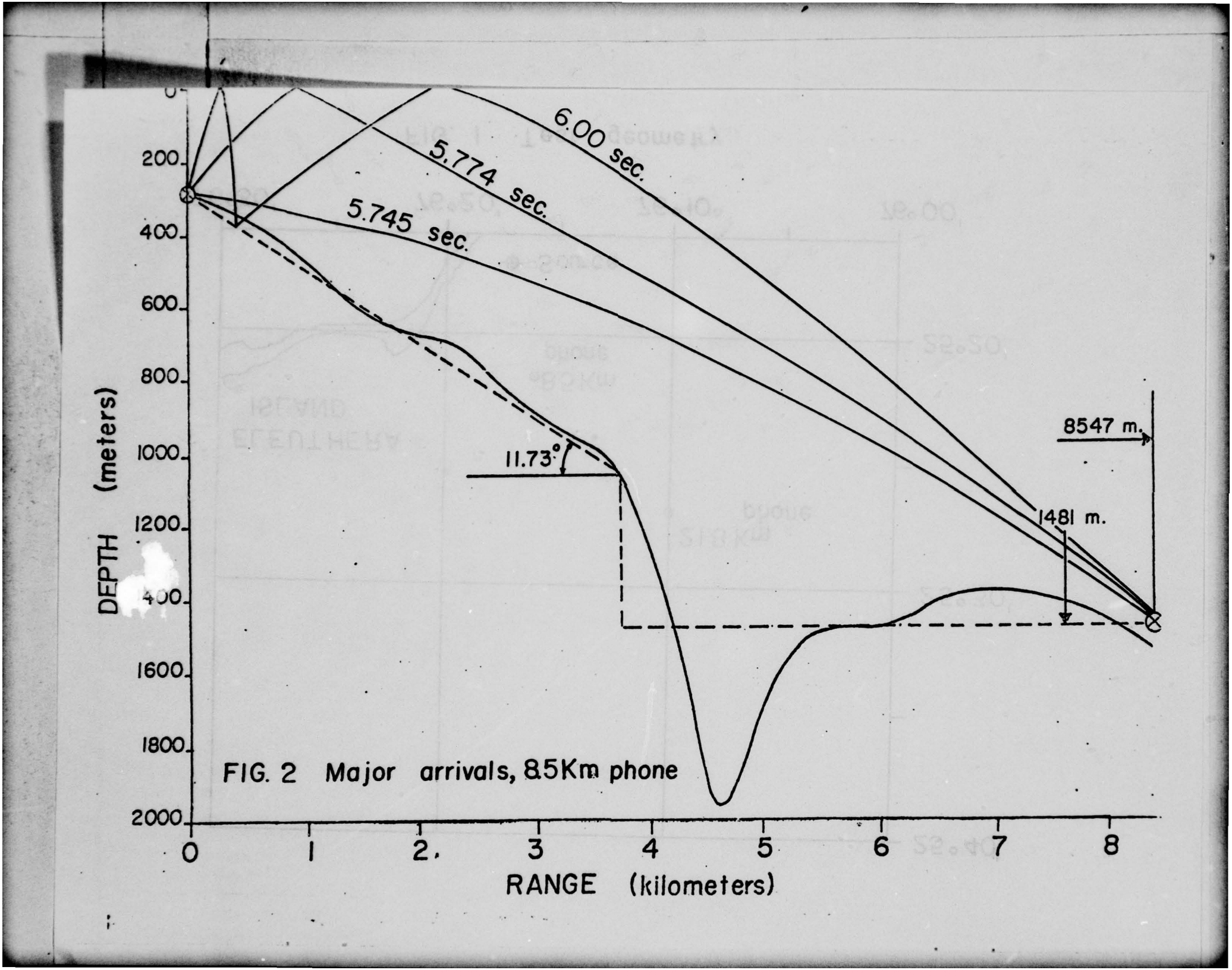

FIG. 2 Major arrivals, 8.5Km phone

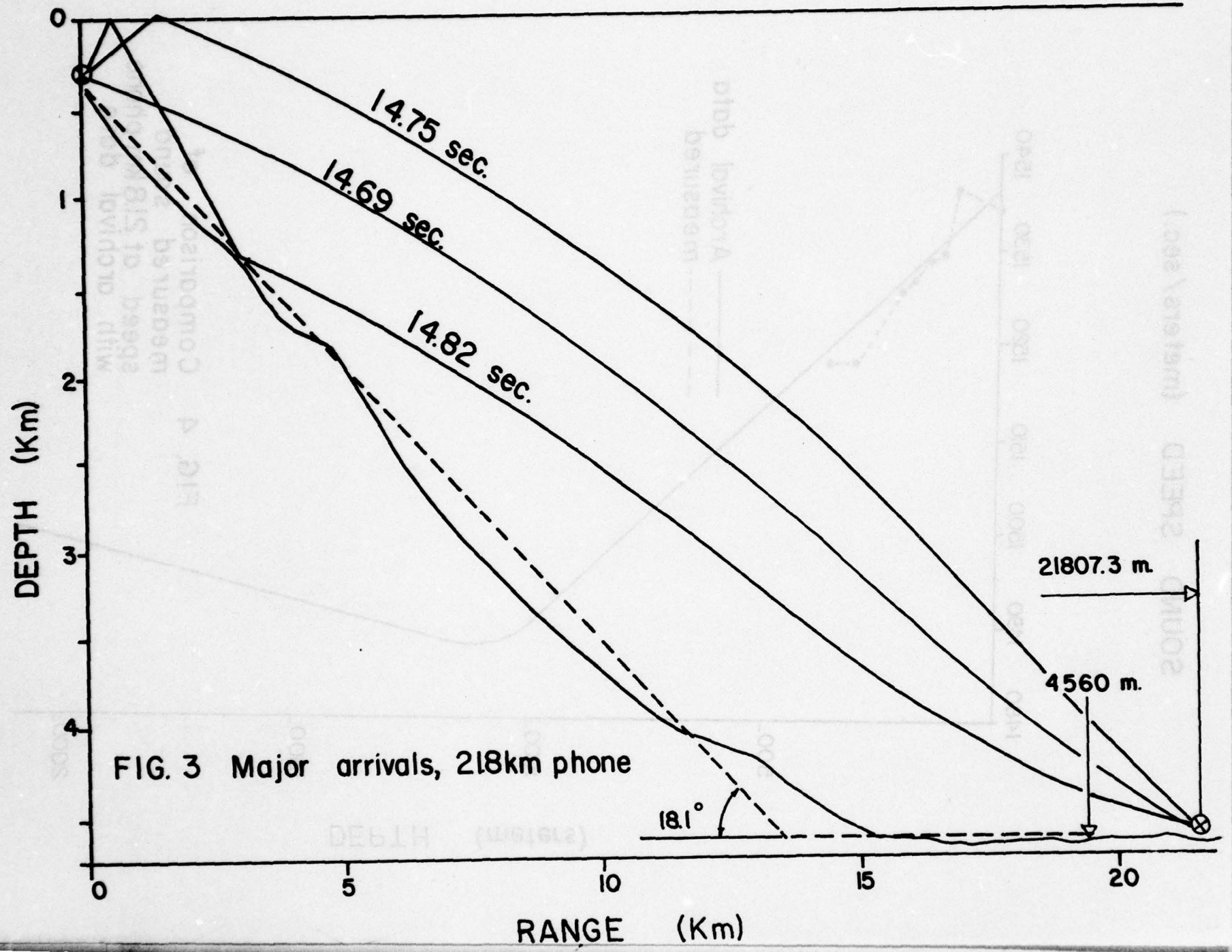

FIG. 3 Major arrivals, 218km phone

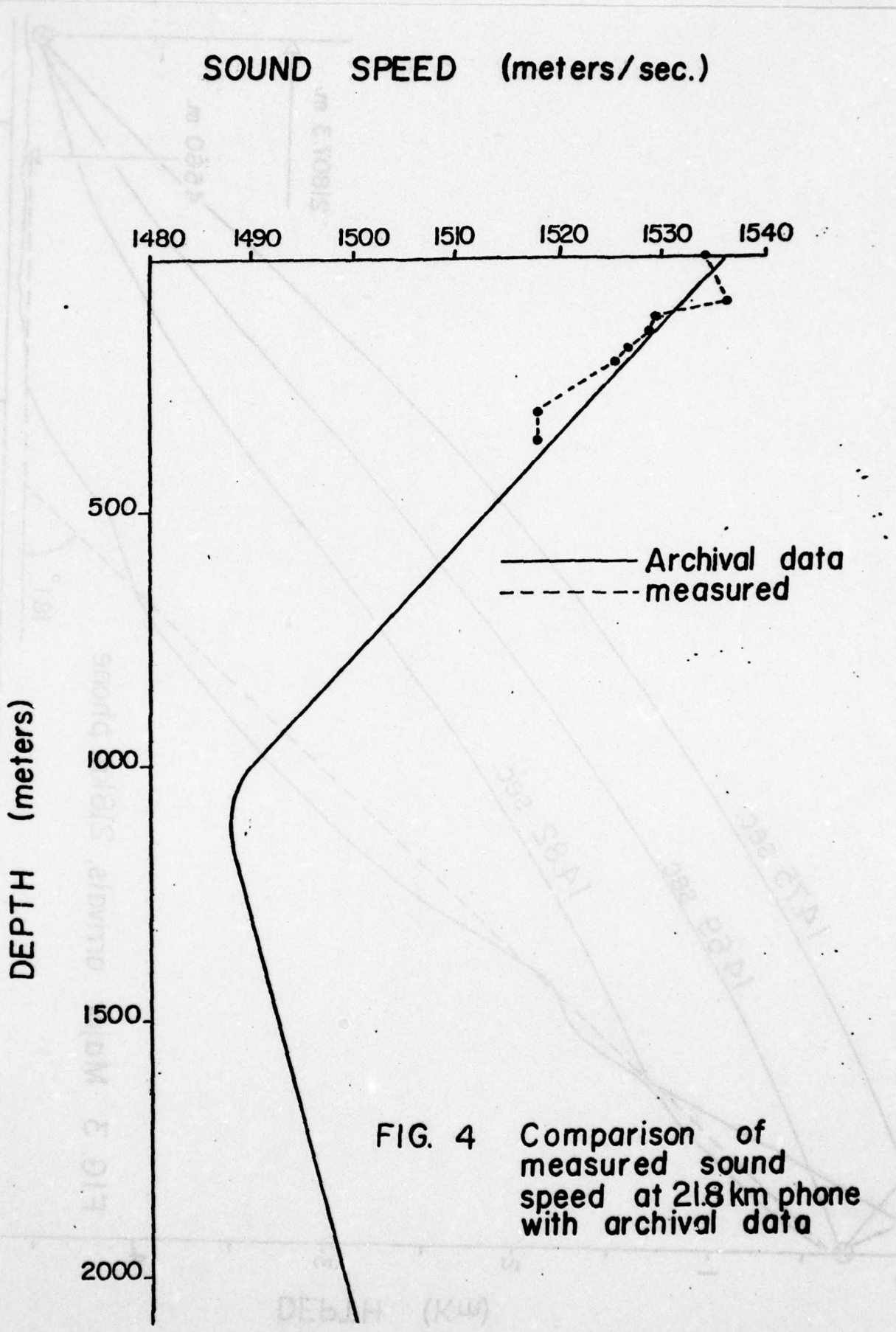

FIG. 4 Comparison of measured sound speed at 21.8 km phone with archival data

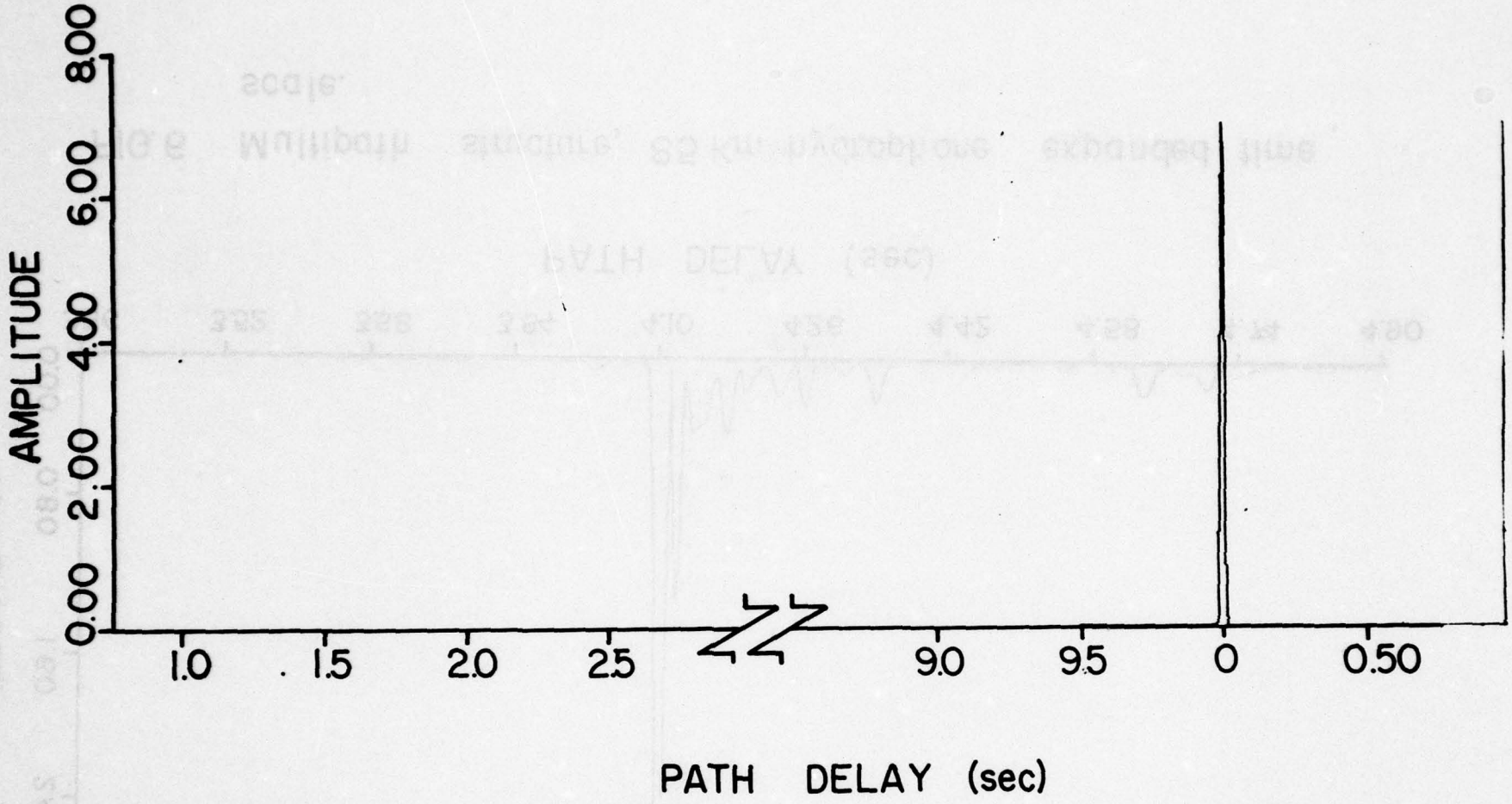

FIG. 5 CALIBRATION CHANNEL FOR MULTIPATH STRUCTURE

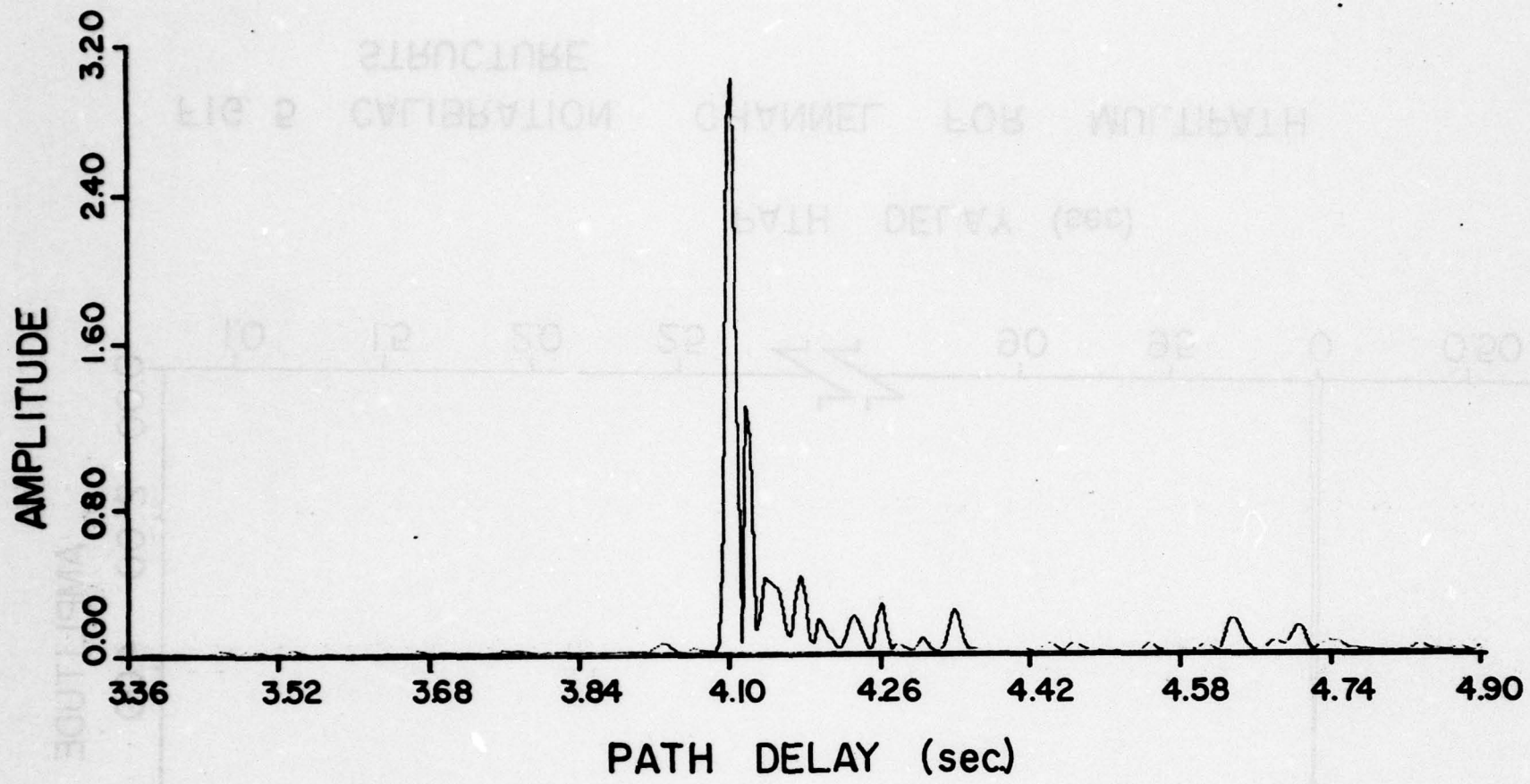

FIG. 6 Multipath structure, 8.5 Km hydrophone expanded time scale.

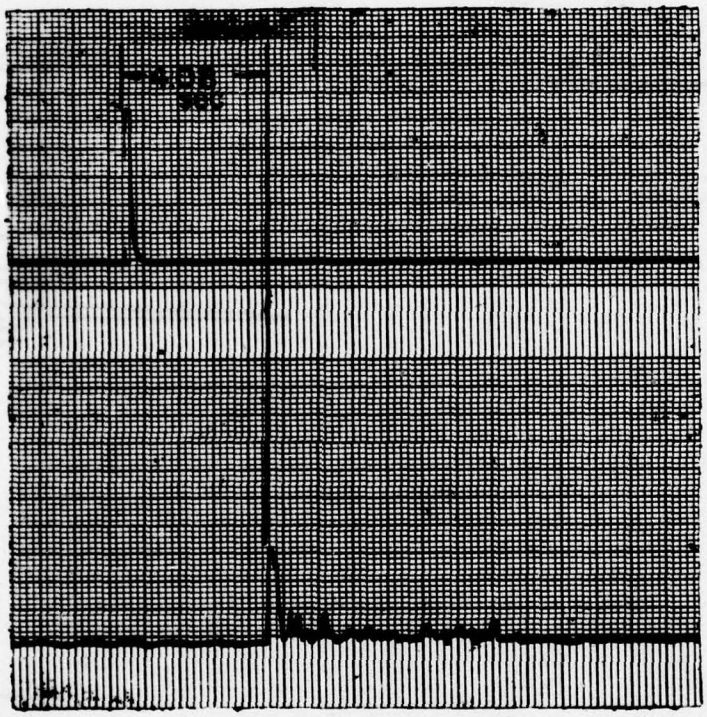

FIG. 8 CHART RECORDER OUTPUT OF PROJECTOR AND 8.5 Km HYDROPHONE

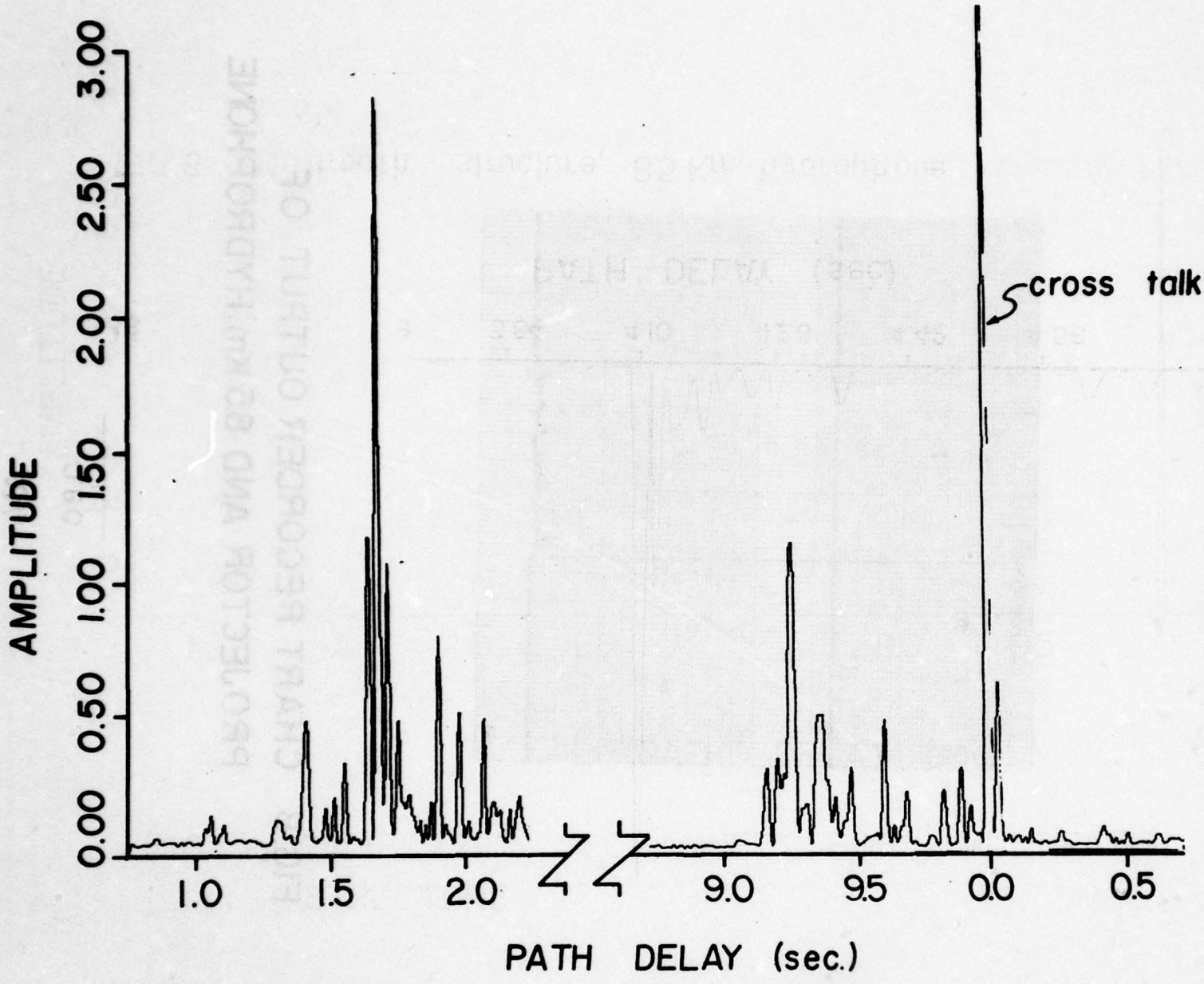

FIG. 7 Multipath structure, 21.8km hydrophone

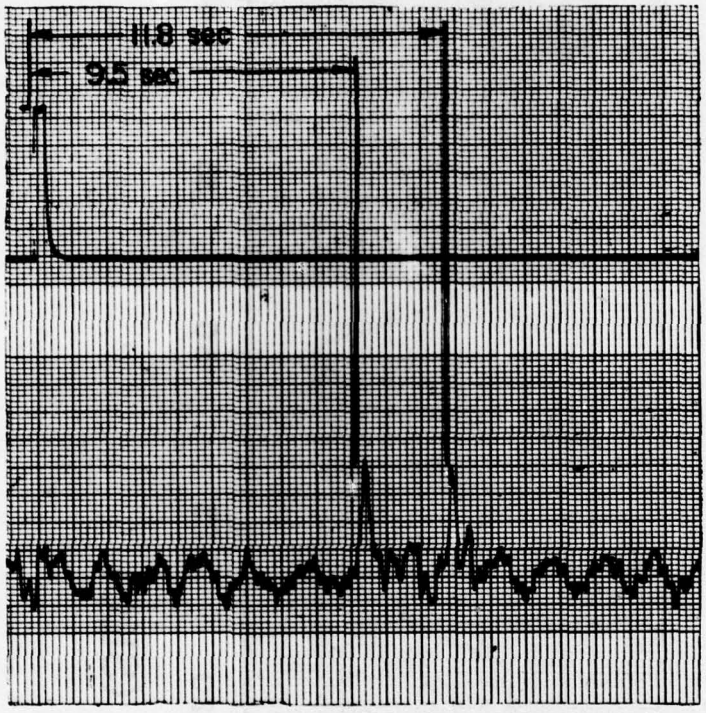

FIG. 9 CHART RECORDER OUTPUT OF PROJECTOR AND 21.8 Km HYDROPHONE

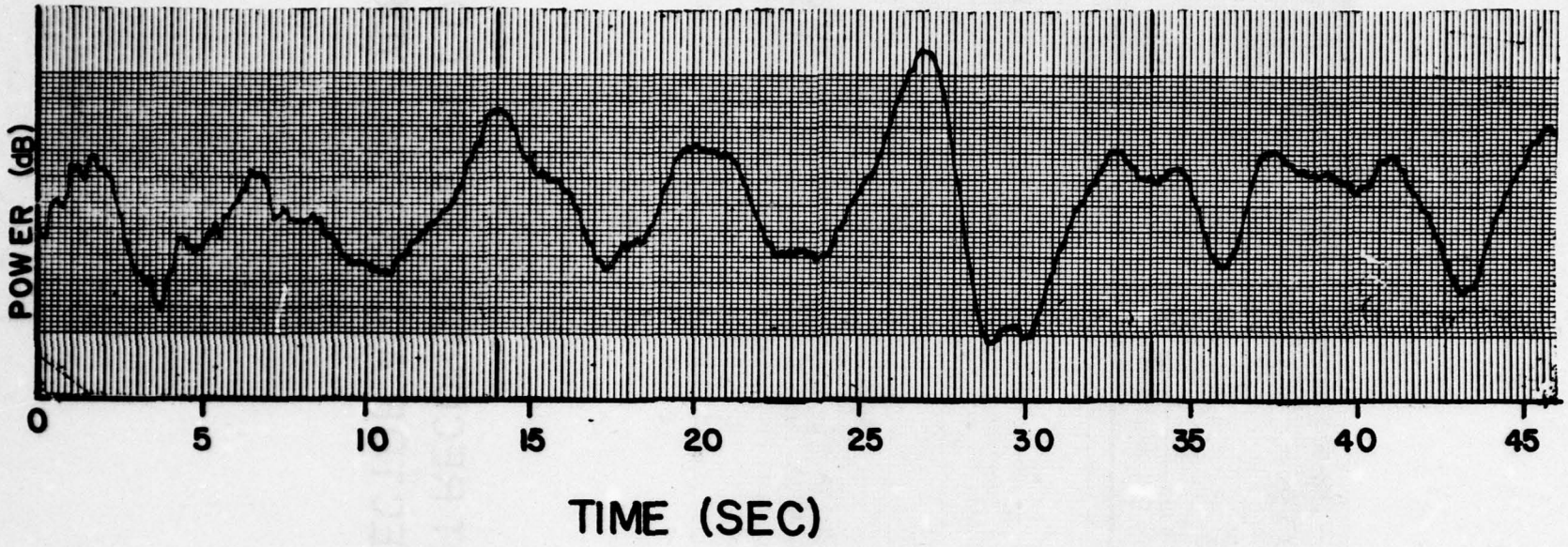

FIG. 10 SURFACE WAVE MODULATION
8.5 Km HYDROPHONE

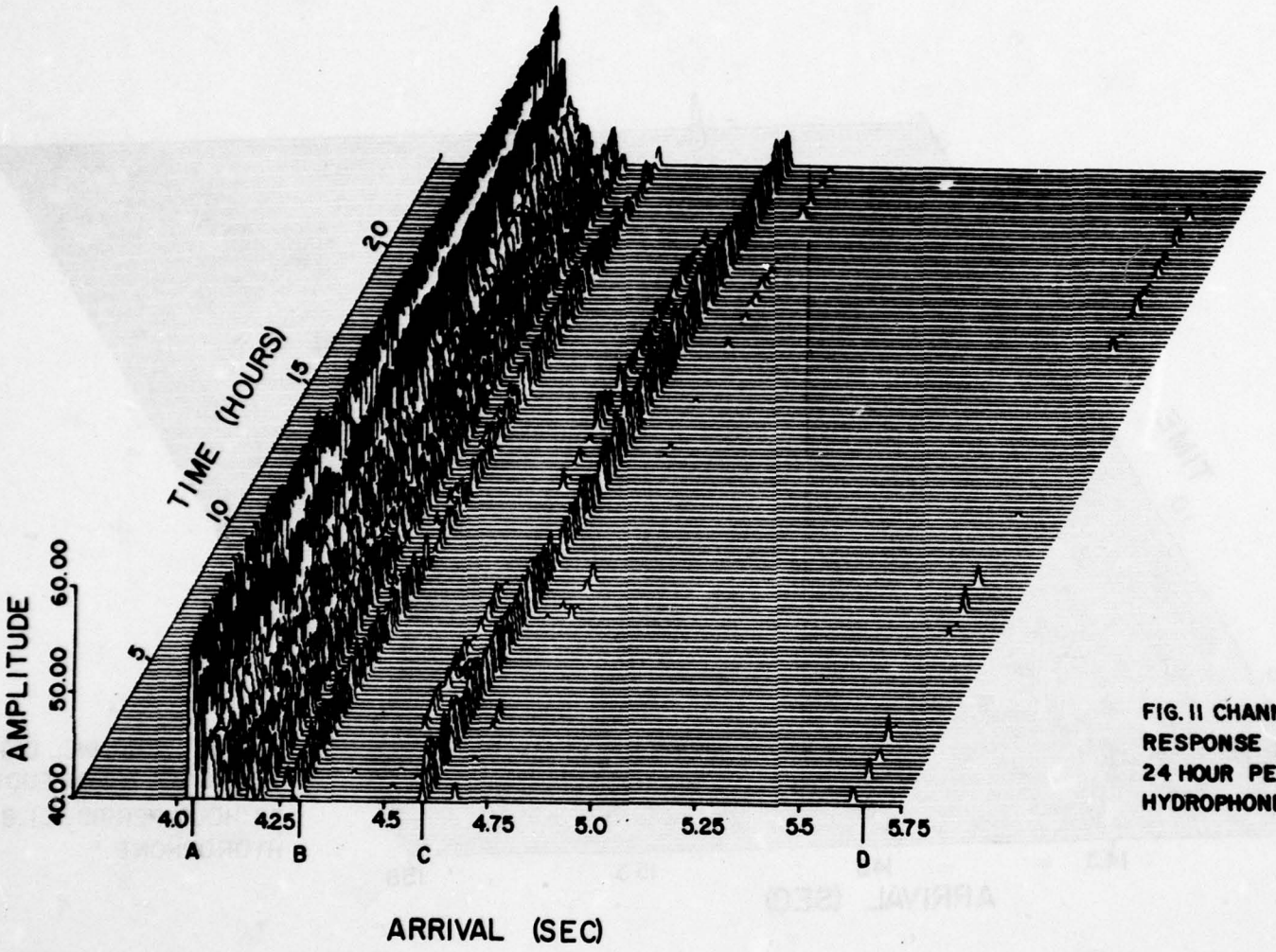

FIG. 11 CHANNEL DIGIT RESPONSE MAGNITUDE FOR 24 HOUR PERIOD, 8.5 Km HYDROPHONE

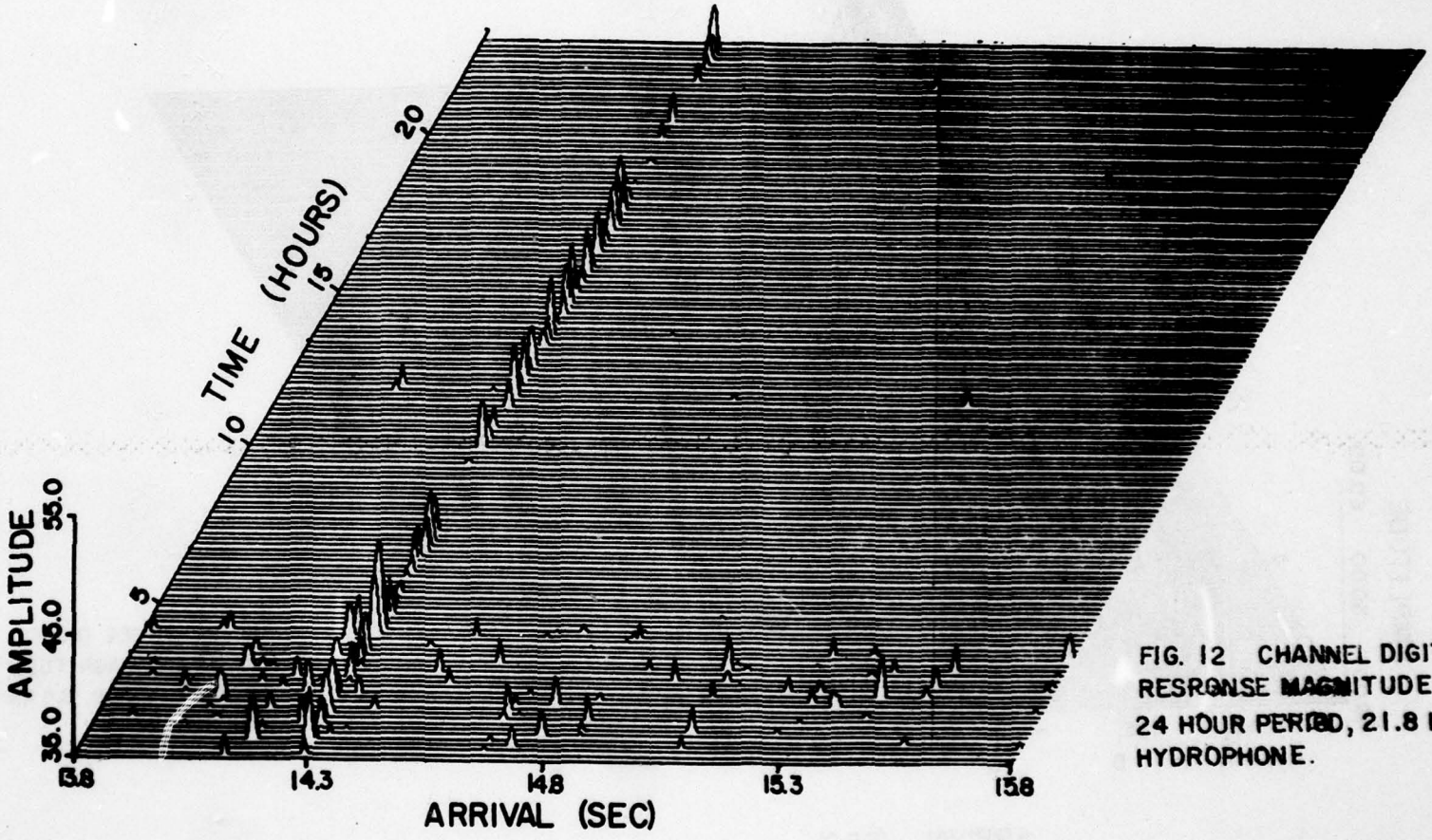

FIG. 12 CHANNEL DIGIT RESPONSE MAGNITUDE FOR 24 HOUR PERIOD, 21.8 Km HYDROPHONE.

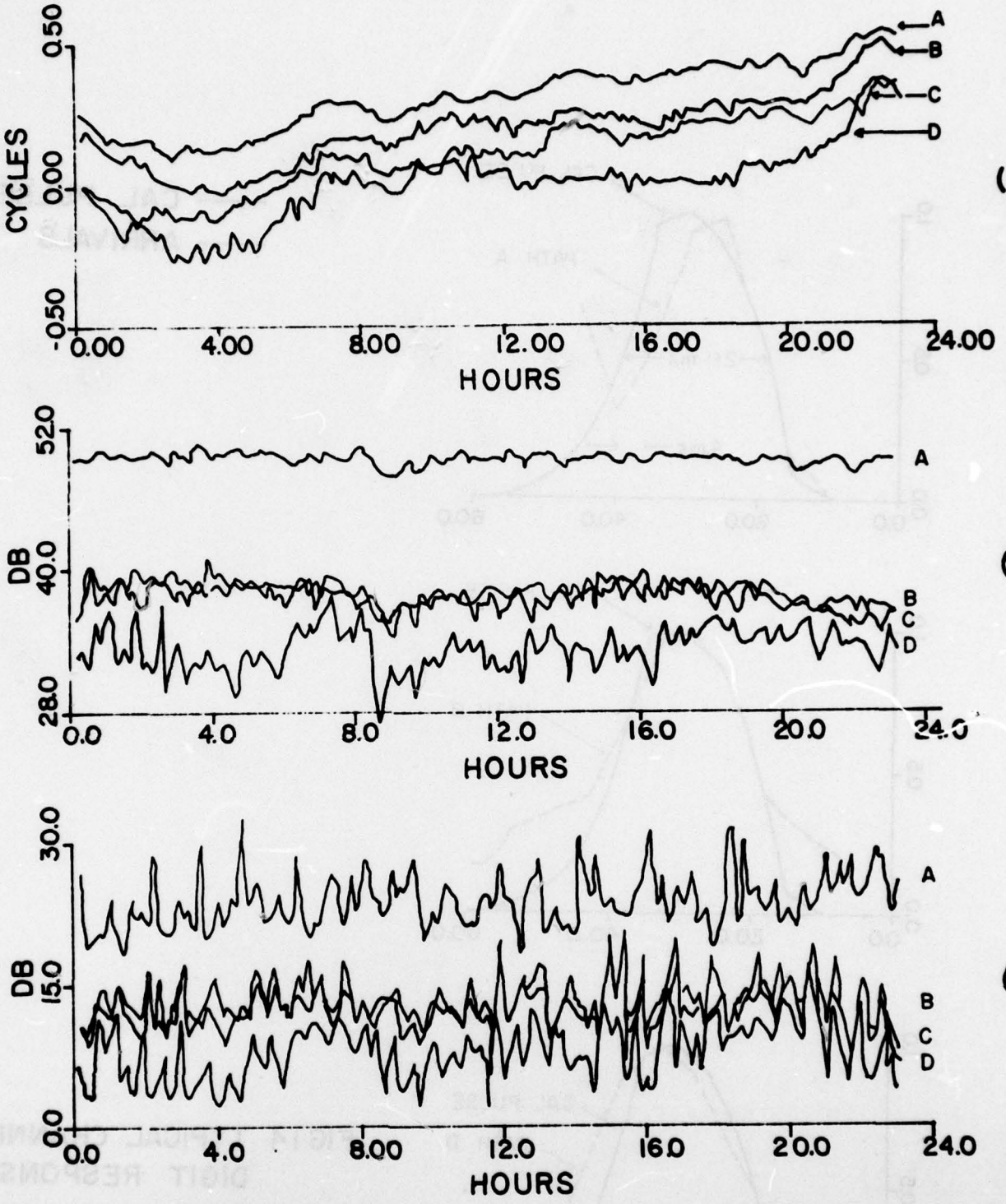

FIG 13 TIME SERIES OF (a) PHASE, (b) AMPLITUDE, AND (c) SIGNAL-TO-NOISE RATIO FOR FOUR SELECTED PATHS, 8.5 Km HYDROPHONE

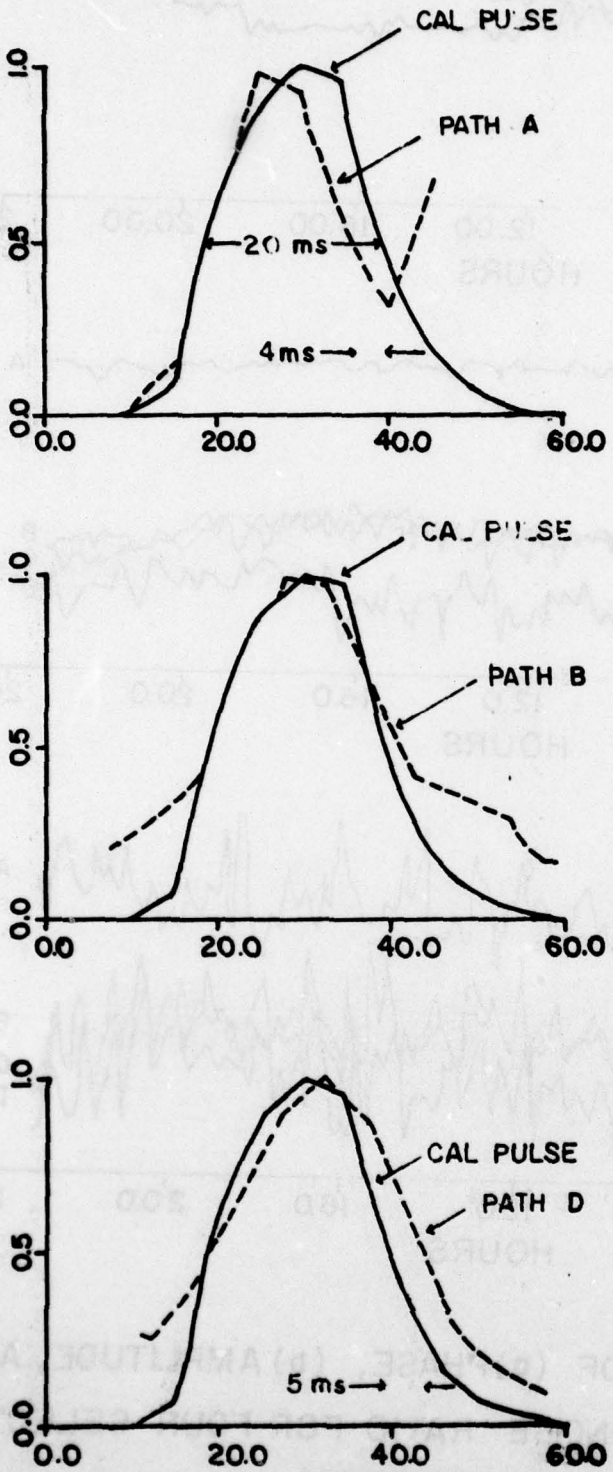

—— CAL PULSE
----- ARRIVALS

FIG 14 TYPICAL CHANNEL DIGIT RESPONSE MAGNITUDE FOR SELECTED PATHS AND FOR CALI - BRATION DIGIT

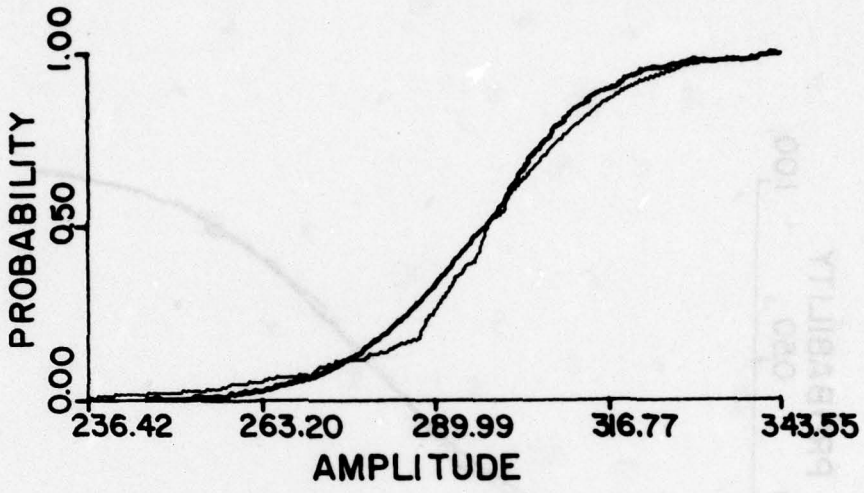

FIG. 15 GOODNESS OF FIT TEST FOR AMPLITUDE, 8.5 Km PHONE, PATH A

—— GAUSSIAN CUMULATIVE DISTRIBUTION

—— EXPERIMENTAL CUMULATIVE DISTRIBUTION

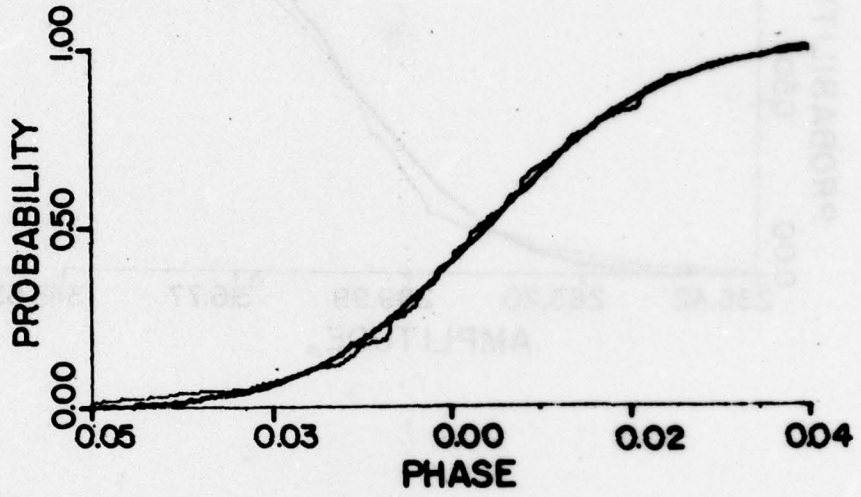

FIG 16 GOODNESS OF FIT TEST FOR PHASE, 8.5 Km. PHONE, PATH A

—— GAUSSIAN CUMULATIVE DISTRIBUTION

—— EXPERIMENTAL CUMULATIVE DISTRIBUTION

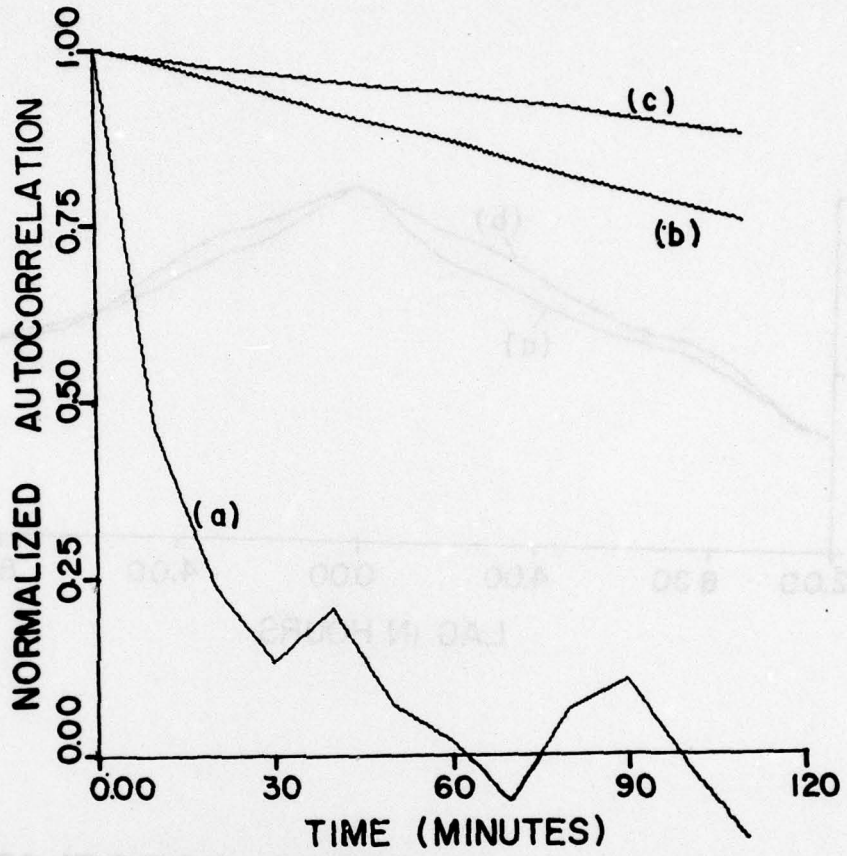

FIG 17 NORMALIZED AUTOCORRELATION FUNCTIONS FOR (a) AMPLITUDE, (b) PHASE, (c) COMPLEX ENVELOPE

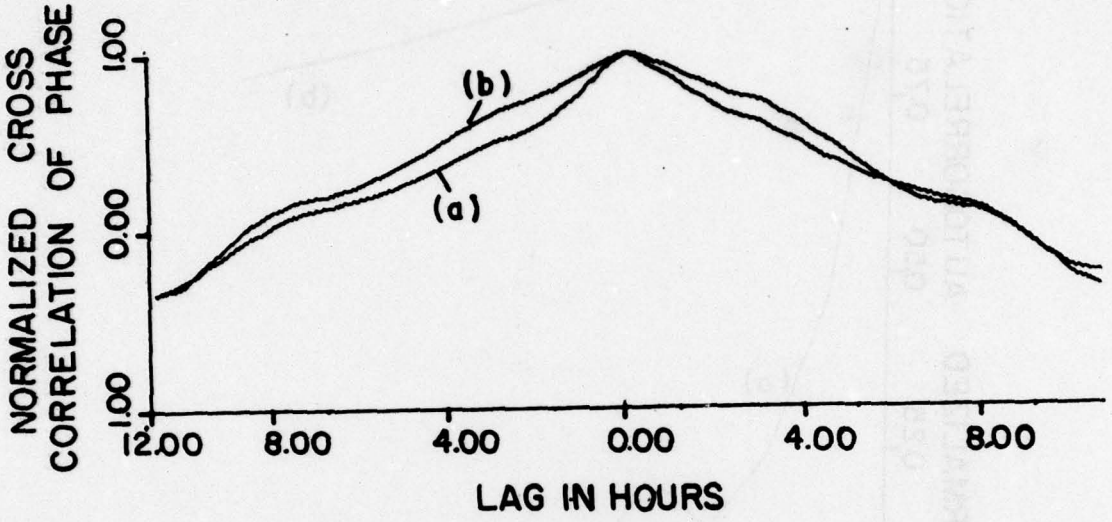

FIG 18 NORMALIZED CROSS CORRELATION OF PHASE FOR SELECTED PATHS 8.5 Km PHONE , (a) PATHS A & B (b) PATHS A & C

DISTRIBUTION LIST

Office of Naval Research
800 N. Quincy Street
Arlington, Virginia 22217
Att: Code 222 — 2
1020S — 1
480 — 1

Director — 6
Naval Research Laboratory
4555 Overlook Avenue S.W.
Washington, D.C. 20375

Director — 1
Office of Naval Research Branch Office
1030 East Green Street
Pasadena, California 91106

Office of Naval Research — 1
San Francisco Area Office
760 Market Street Room 447
San Francisco, California 94102

Director — 1
Office of Naval Research Branch Office
495 Summer Street
Boston, Massachusetts 02210

Office of Naval Research — 1
New York Area Office
207 West 24th Street
New York, N.Y. 10011

Commanding Officer — 1
Office of Naval Research Branch Office
Box 39
FPO New York 09510

Director — 1
Office of Naval Research Branch Office
536 South Clark Street
Chicago, Illinois 60606

Commander — 1
Naval Surface Weapons Center
Acoustics Division
Silver Spring, Maryland 20910
Att: Dr. Zaka Slawsky

Naval Oceanographic Office — 1
NSTL Station
Bay St. Louis, Miss. 39520
Att: Mr. W. Geddes

Officer in Charge 1
Naval Ship R&D Center
Annapolis Laboratory
Annapolis, Maryland 21402

Commander
Naval Sea Systems Command
National Center #2
2521 Jefferson Davis Highway
Arlington, Virginia 20360
Att: SEA 037 1
Carey Smith, 06H1 1
David F. Bolka, 06H2 1

Commanding Officer 1
Fleet Numerical Weather Center
Monterey, Calif. 93940

Defense Documentation Center 12
Cameron Station
Alexandria, Virginia 22314

Director of Navy Laboratories 1
Chief of Naval Material
2211 Jefferson Davis Highway
Crystal Plaza #5
Arlington, Virginia 20360
Att: Dr. James Probus, MAT 03L

Commander 1
Naval Electronic Systems Command
2511 Jefferson Davis Highway
National Center #1
Arlington, Virginia 20360
Att: CDR A.R. Miller, ELEX 320

Commander 2
Naval Ship R&D Center
Dept. of the Navy
Bethesda, Maryland 20084
Att: Mr. Craig Olson
Uncl. Library

Chief of Naval Operations 1
Room 4D518, Pentagon
Washington, D.C. 20350
Att: Capt. A.H. Gilmore

Commander 3
Naval Ocean Systems Center
Dept. of the Navy
San Diego, Calif. 92132
Att: Dr. Dan Andrews
Dr. Dean Hanna
Mr. Henry Aurand

Superintendent 1
Naval Research Laboratory
Underwater Sound Reference Division
P.O. Box 8337
Orlando, Fla. 32806

Commanding Officer 3
Naval Underwater Systems Center
New London Laboratory
New London, Conn. 06320
Att: Dr. A. Nuttall
Mr. A. Ellinthorpe
Dr. D.M. Viccione

Commander 1
Naval Air Development Center
Dept. of the Navy
Warminster, Pennsylvania 18974
Att: Unclass. Library

Superintendent 1
Naval Postgraduate School
Monterey, Calif. 93940
Att: Unclass. Library

Commanding Officer 1
Naval Coastal Systems Laboratory
Panama City, Fla. 32401
Att: Unclass. Library

Commanding Officer 1
Naval Underwater Systems Center
Newport Laboratory
Newport, Rhode Island 02840
Att: Unclass. Library

Superintendent 1
U.S. Naval Academy
Annapolis, Maryland 21402
Att: Library

Commanding Officer 2
Naval Intelligence Support Center
4301 Suitland Road
Suitland, Maryland 20390
Att: Dr. Johann Martinek
Mr. E. Bissett

Commander 1
Naval Sea Systems Command
Washington, D.C. 20362
Att: Uncl. Library, SEA 03E

Special Assistant for ASW 1
Office of the Assistant Secretary of
the Navy for Research, Engineering
& Systems
Washington, D.C. 20350
Att: Dr. D. Hyde

Dr. Melvin J. Jacobson 1
Rensselaer Polytechnic Inst.
Troy, New York 12181

Dr. T.G. Birdsall 1
Cooley Electronics Laboratory
University of Michigan
Ann Arbor, Michigan 48105

Dr. Harry DeFerrari 1
University of Miami
Rosenstiel School of Marine Science
4600 Rickenbacker Causeway
Miami, Florida 33149

Dr. M.A. Basin 1
S.D.P. Inc
15250 Ventura Blvd
Suite 518
Sherman Oaks, Calif 91403

Dr. Walter Duing 1
University of Miami
Rosenstiel School of Marine Sciences
4600 Rickenbacker Causeway
Miami, Fla. 33149

Dr. David Middleton 1
127 East 91st Street
New York, N.Y. 10028

Dr. Donald Tufts 1
University of Rhode Island
Kingston, Rhode Island 02881

Dr. Loren Nolte 1
Duke University
Dept. of Electrical Eng.
Durham, N. Carolina 27706

Mr. S.W. Autrey 1
Hughes Aircraft Company
P.O. Box 3310
Fullerton, Calif. 92634

Dr. Richard W. James 1
c/o Fleet Weather Facility
4031 Suitland Rd.
Washington, D.C. 20390

Dr. Thomas W. Ellis 1
Texas Instruments, Inc.
13500 North Central Expressway
Dallas, Texas 75231

Dr. Terry Ewart 1
Applied Physics Lab.
University of Washington
1013 N.E. 40th Street
Seattle, Wash., 98195

Institute for Acoustical Research 2
Miami Div. of Palisades Geophysical Inst.
615 S.W. 2nd Avenue
Miami, Fla. 33130
Att: Mr. M. Kronengold
Dr. J. Clark
Dr. W. Jobst

Mr. Carl Hartdegen 1
Palisades Sofar Station
Bermuda Div. of Palisades Geophysical Inst.
FPO New York 09560

Mr. Beaumont Buck 1
Polar Research Lab.
123 Santa Barbara Avenue
Santa Barbara, Calif 93101

Dr. M. Weinstein 1
Underwater Systems Inc.
8121 Georgia Avenue
Silver Spring, Maryland 20910

Applied Research Laboratories 2
Univ. of Texas at Austin
P.O. Box 8029
10000 FM Road 1325
Austin, Texas 78712
Att: Dr. Lloyd Hampton
Dr. Charles Wood

Dr. C.N.K. Mooers 1
University of Delaware
Newark, Delaware 19711

Woods Hole Oceanographic Inst. 1
Woods Hole, Massachusetts 02543
Att: Dr. Paul McElroy

Dr. John Bouyoucos 1
Hydroacoustics, Inc.
321 Northland Avenue
P.O. Box 3818
Rochester, N.Y. 14610

Atlantic Oceanographic & Meteorological Lab. 1
15 Rickenbacker Causeway
Miami, Fla. 33149
Att: Dr. John Proni

S.A.I. Inc. 1
8400 Westpark Drive
McClean, Virginia 22102
Att: Ms. Angela D'Amico
Ms. Lorna Blumen

Commanding Officer 1
U.S. Naval Facility
FPO, New York 09556

Dr. Victor C. Anderson 1
Marine Physical Lab.
Scripps Inst. of Oceanography
University of California
La Jolla, Calif. 92037

Office of Naval Research 1
Resident Rep.
Lamont-Doherty Geological Observatory
Palisades, New York 10964

Advanced Research Projects Agency 1
(ARPA)
1400 Wilson Blvd.
Arlington, Va. 22209
Att: Dr. R. Gustafson

Naval Air Development Center 1
Warminster, Pa. 18974
Att: Keith Jerome, Proj. Eng.

Ocean Systems Pacific 1
Box 1309
FPO San Francisco 96610
Att: LCDR F.T. Gray
Lt. William Johnston

Commander Oceanographic Systems 1
Atlantic (COSL)
Box 100
Norfolk, Va.

NORDA 1
NSTL Station
Bay St. Louis, Miss., 39520
Att: M.G. Lewis

UNCLASSIFIED

SECURITY CLASSIFICATION OF THIS PAGE (When Data Entered)

REPORT DOCUMENTATION PAGE	READ INSTRUCTIONS BEFORE COMPLETING FORM
1. REPORT NUMBER: 79001	2. GOVT ACCESSION NO. / 3. RECIPIENT'S CATALOG NUMBER
4. TITLE (and Subtitle): EXPERIMENTAL EVIDENCE OF THE IMPORTANCE OF SUB-BOTTOM REFRACTION AT 206 HZ.	5. TYPE OF REPORT & PERIOD COVERED: Final Report. / 6. PERFORMING ORG. REPORT NUMBER
7. AUTHOR(s): Benjamin Rosenberg, Luciano Dominijanni, William Jobst	8. CONTRACT OR GRANT NUMBER(s): N62269-75-C-0305
9. PERFORMING ORGANIZATION NAME AND ADDRESS: Institute for Acoustical Research, 615 S.W. 2nd Avenue, Miami, Fla. 33130	10. PROGRAM ELEMENT, PROJECT, TASK AREA & WORK UNIT NUMBERS
11. CONTROLLING OFFICE NAME AND ADDRESS: Procuring Contracting Officer, Naval Air Development Center, Warminster, Pa. 18974	12. REPORT DATE: Sept[illegible]78 / 13. NUMBER OF PAGES: 50 (55 p.)
14. MONITORING AGENCY NAME & ADDRESS (if different from Controlling Office): Office of Naval Research Resident Rep., Columbia University, Lamont Doherty Geological Observatory, Torrey Cliff, Palisades, New York 10913	15. SECURITY CLASS. (of this report): Unclassified / 15a. DECLASSIFICATION/DOWNGRADING SCHEDULE
16. DISTRIBUTION STATEMENT (of this Report): Distribution of this Document is unlimited (14) EAR-7900	
17. DISTRIBUTION STATEMENT (of the abstract entered in Block 20, if different from Report)	
18. SUPPLEMENTARY NOTES	
19. KEY WORDS (Continue on reverse side if necessary and identify by block number): Acoustic propagation; Bottom propagated paths; Channel impulse response	

20. ABSTRACT (Continue on reverse side if necessary and identify by block number)

Acoustic data obtained using a bottom mounted 206 Hz projector and two bottom mounted receiving hydrophones 8.5 km and 21.8 km distant showed multiple acoustic paths with travel times approximately 30 percent faster than predicted for water-borne propagation. The presence of amplitude modulation with a 6.5 second period indicated that acoustic energy was reflected from the ocean surface before entering the high velocity limestone CONT'

DD FORM 1 JAN 73 1473 EDITION OF 1 NOV 65 IS OBSOLETE S/N 0102-014-6601

408144 R.F. R.L.H.

UNCLASSIFIED

SECURITY CLASSIFICATION OF THIS PAGE (When Data Entered)

Cont

and coral bottom and being refracted to the receivers. Since received pulses showed little distortion, sub-bottom layers may be modeled as complex impedances at the 206 Hz frequency. The results demonstrate the importance of bottom propagated energy at low frequency and short range.